Published in final edited form as:
Cancer Discov. 2012 October ; 2(10): 906–921. doi:10.1158/2159-8290.CD-12-0085.

VEGF/Neuropilin-2 Regulation of Bmi-1 and Consequent Repression of IGF-1R Define a Novel Mechanism of Aggressive Prostate Cancer

Hira Lal Goel[1,9], **Cheng Chang**[1], **Bryan Pursell**[1], **Irwin Leav**[1], **Stephen Lyle**[1], **Hualin Simon Xi**[2], **Chung-Cheng Hsieh**[1], **Helty Adisetiyo**[3], **Pradip Roy-Burman**[3], **Ilsa M. Coleman**[4], **Peter S. Nelson**[4,5,6], **Robert L. Vessella**[5,6], **Roger J. Davis**[8], **Stephen R. Plymate**[5,6,7], and **Arthur M. Mercurio**[1]

[1]Department of Cancer Biology, University of Massachusetts Medical School, Worcester, MA

[2]Bioinformatics Core, University of Massachusetts Medical School, Worcester, MA

[3]Department of Pathology, Keck School of Medicine, University of Southern California, Los Angeles, CA

[4]Division of Human Biology, Fred Hutchinson Cancer Research Center, Seattle, WA

[5]Department of Urology, University of Washington School of Medicine, Seattle, WA

[6]Department of Medicine, University of Washington School of Medicine, Seattle, WA

[7]Geriatric Research, Education and Clinical Center, Veterans Affairs Puget Sound Health Care System, Seattle, WA

[8]Howard Hughes Medical Institute and Program in Molecular Medicine, University of Massachusetts Medical School, Worcester, MA

Abstract

We demonstrate that the VEGF receptor, neuropilin-2 (NRP2) is associated with high-grade, PTEN-null prostate cancer and that its expression in tumor cells is induced by PTEN loss as a consequence of c-Jun activation. VEGF/NRP2 signaling represses IGF-1R expression and signaling and the mechanism involves Bmi-1-mediated transcriptional repression of the IGF-1R. This mechanism has significant functional and therapeutic implications that were evaluated. IGF-1R expression correlates with PTEN and inversely with NRP2 in prostate tumors. NRP2 is a robust biomarker for predicting response to IGF-1R therapy because prostate carcinomas that express NRP2 exhibit low levels of IGF-1R. Conversely, targeting NRP2 is only modestly effective because NRP2 inhibition induces compensatory IGF-1R signaling. Inhibition of both NRP2 and IGF-1R, however, completely blocks tumor growth *in vivo*.

[9]Corresponding author: Hira Lal Goel, Ph.D. Department of Cancer Biology University of Massachusetts Medical School LRB-470 364 Plantation Street Worcester, MA 01605 phone: 508-856-1936 fax: 508-856-1310 hira.goel@umassmed.edu.

Disclosure of Potential Conflict of Interest: Authors declare no potential conflict of interest.

Keywords

Prostate Cancer; VEGF; Neuropilin; IGF-1R; Bmi-1; PTEN

INTRODUCTION

Understanding mechanisms that drive the initiation and progression of prostate cancer is essential to improving the clinical management of this disease, which is the most common cancer in men in the United States and Western Europe (1). Although early stage prostate cancer can be treated reasonably well clinically, advanced forms of this disease are very aggressive and difficult to manage with existing therapies. As a consequence, these tumors are associated with a high degree of morbidity and mortality. Our approach to understanding the biology of aggressive prostate cancer is rooted in the hypothesis that tumor cells express receptors for VEGF and that VEGF signaling in tumor cells contributes to tumor formation and progression (2-5). Surprisingly, however, little is known about the expression and function of VEGF receptors on prostate carcinoma cells and their contribution to this disease. This problem is significant because these receptors and the signaling pathways that they regulate are prime targets for therapeutic intervention.

The neuropilins (NRPs) are one class of VEGF receptors that are particularly interesting with respect to cancer biology. NRP1 and NRP2 were identified initially as neuronal receptors for semaphorins, which are axon guidance factors that function primarily in the developing nervous system (6, 7). The seminal finding by Klagsbrun that neuropilins can also function as VEGF receptors and that they are expressed on endothelial and tumor cells launched studies aimed at understanding their functional contribution to angiogenesis and tumor biology (8). NRPs have the ability to interact with and modulate the function of tyrosine kinase VEGF receptors (VEGFR1 and VEGFR2), as well as other receptors (9, 10). There is also evidence that NRPs can function independently of other receptors (11) and that they are valid targets for therapeutic inhibition of angiogenesis and cancer (12-14).

This study demonstrates that the expression of NRP2 in prostate cancer cells is induced by PTEN deletion and that its expression correlates with Gleason grade. Given that the inactivation of PTEN is one of the most common genetic lesions in prostate cancer and its frequency increases with more aggressive disease (15), our discovery led to the hypothesis that VEGF/NRP2 signaling in tumor cells has a key role in prostate carcinogenesis. Indeed, the data obtained reveal that VEGF/NRP2 signaling contributes to the expression of Bmi-1, a Polycomb group transcriptional repressor that has been implicated in the etiology of prostate cancer induced by PTEN deletion (16). We also discovered that Bmi-1 represses transcription of the IGF-1 receptor (IGF-1R), which is relevant because IGF-1R signaling contributes to tumor growth (17) and the IGF-1R is a potential therapeutic target for prostate cancer (18). We conclude from our data that aggressive prostate cancer cells exhibit VEGF/NRP2 signaling, Bmi-1 expression and reduced IGF-1R expression. The functional and therapeutic implications of these findings were evaluated, and the results highlight a novel role for NRP2 as a biomarker for predicting response to IGF-1R therapy and as a therapeutic target itself in combination with IGF-1R inhibition.

RESULTS

NRP2 is induced in prostate cancer as a consequence of PTEN loss and JNK1/c-Jun activation

Although aggressive prostate cancer is characterized by elevated VEGF expression in tumor cells (19, 20), therapeutic approaches based on VEGF inhibition have been largely unsuccessful. Bevacizumab, a VEGF antibody, did not impact patients with metastatic, castration-resistant prostate cancer and the trial was halted because it did not meet pre-defined response goals (21). Bevacizumab, however, does not inhibit the interaction of VEGF with the VEGF receptor NRP2 (22), which is noteworthy because we observed that NRP2 expression is induced in prostate cancer and that it correlates with Gleason grade (Fig. 1A-B). Specifically, there is no significant NRP2 expression in normal, immortalized prostate cell lines, normal prostatic epithelium or PIN (Fig. 1A-C). The expression of NRP2 in prostate cancer cell lines correlates with their invasive potential (Fig. 1A and Supplementary Fig. 1A). Robust NRP2 expression is seen in high-grade prostate cancer (Gleason grade 5) and metastases compared to low-grade prostate cancer (Gleason grade 3) (Fig. 1B-C, Supplementary Fig. 1B-D). Importantly, NRP2 expression in prostate cancer correlates significantly with grade ($p<0.001$) and clinical outcome ($p=0.047$) (Supplementary Fig. 2A-D). Prostate carcinoma cells also express VEGFR2 but lack expression of VEGFR1 (Supplementary Fig. 2E) (23, 24).

Given that PTEN loss has a causative role in the genesis of aggressive prostate cancer and correlates with Gleason grade (15, 25), we assessed the association of NRP2 expression with PTEN loss and observed a striking correlation. Relatively high NRP2 expression is seen in high Gleason grade tumors and metastases, which exhibit frequent PTEN loss (15, 25) (Fig. 1B). Interestingly, however, there is heterogeneity in NRP2 expression in Gleason grade 3 prostate cancer specimens, where approximately 12.5% of the cases expressed high levels of NRP2 (expression levels 4 and 5) (Fig. 1B, Supplementary Fig. 2A-D). Gleason grade 3 tumors that harbored a PTEN deletion were positive for NRP2 expression but those tumors that expressed PTEN were negative for NRP2 (Fig. 2A). These data are consistent with the finding that PTEN loss occurs in approximately 15-20% of low-grade prostate cancer (15, 25). The association between PTEN loss and NRP2 expression was substantiated by analyzing prostate tumors in $PTEN^{pc-/-}$ mice, which are invasive and aggressive (26). These tumors display relatively high NRP2 expression compared to the mouse prostatic epithelium (Fig. 2B). NRP2 expression is also high in PIN lesions in the $PTEN^{pc-/-}$ mice consistent with the hypothesis that PTEN loss induces NRP2 (Fig. 2B). This consequence of PTEN loss is specific to NRP2 because NRP1 is expressed in both normal prostate epithelium and $PTEN^{pc-/-}$ tumors (Fig. 2B, Supplementary Fig. 3A). These results imply that PTEN represses NRP2 but not NRP1 expression. To test this hypothesis, PTEN was expressed in PC3 and C4-2 cells, which are PTEN-null and express NRP2. PTEN expression ablated NRP2 expression and the activity of a NRP2 promoter reporter construct but it had no effect on NRP1 expression (Fig. 2C-E). These results indicate that NRP2 is associated with aggressive, PTEN-null prostate cancer. Importantly, NRP2 expression is not a function of tumor differentiation because of the heterogeneity of its expression in Grade 3 tumors, which are all differentiated, and our observation that NRP2 is not expressed in VCaP cells,

which are poorly differentiated but PTEN-positive (Fig. 2D). DU145 cells, which are PTEN-positive, also lack NRP2 (Fig. 2D). Additional evidence to support the conclusion that PTEN loss or inactivation induces NRP2 was obtained by evaluating AKT activation because it is a read-out of PTEN deletion and mutation (27). Indeed, a significant correlation between p-AKT and NRP2 expression was observed in prostate tumors (Supplementary Fig. 3B-C).

To investigate the mechanism behind PTEN-mediated NRP2 suppression, we analyzed the role of c-Jun because it is activated upon PTEN deletion in prostate tumors and contributes to tumorigenesis (28, 29). A significant down-regulation of c-Jun occurred upon PTEN expression in PC3 and C4-2 cells (Fig. 2E-F), and PTEN expression inhibited the activity of a c-Jun promoter and AP1 reporter constructs significantly (Fig. 2G). However, PTEN expression did not affect Coup-TFII, a transcription factor previously shown to regulate NRP2 in lymphatic vessel development (30) (Fig. 2F). We established the role of c-Jun in the regulation of NRP2 using c-Jun shRNAs and TAM67 (a dominant negative c-Jun). Expression of either c-Jun shRNAs or TAM67 reduced NRP2 protein and mRNA levels, as well as NRP2 promoter activity (Fig. 3A-B). Also, an increase in NRP2 promoter activity upon c-Jun over-expression was observed in PC3 and C4-2 cells (Fig. 3C). These results indicate that PTEN represses NRP2 expression by inhibiting c-Jun. We assessed this hypothesis by demonstrating that c-Jun expression rescued NRP2 expression in PC3 and C4-2 cells that had been transfected with a PTEN construct (Fig. 3D). Moreover, our analysis of recently published gene expression data derived from PTEN induction in *Pten*$^{-/-}$ cells (29) revealed an inverse correlation between c-Jun and PTEN, and NRP2 and PTEN expression (Fig. 3E).

To investigate the regulation of NRP2 by c-Jun more rigorously, we performed ChIP and observed that c-Jun binds directly to distinct sites in the NRP2 promoter (Fig. 3F-G). More specifically, the NRP2 promoter contains two AP1 binding sites located within NP3 and NP7 (Fig. 3F) and ChIP confirmed binding to these sites (Fig. 3G). In addition, mutating these sites inhibited NRP2 promoter activity (Supplementary Fig. 4A). As further proof that PTEN represses NRP2 expression by a c-Jun-dependent mechanism, we observed that PTEN significantly inhibited the binding of c-Jun to the NRP2 promoter (Fig. 3H). Given that JNKs are the upstream kinases that regulate c-Jun activity (31), we found that either a dominant-negative JNK or a JNK1 shRNA, but not a JNK2 shRNA inhibited NRP2 expression (Supplementary Fig. 4B-D).

NRP2 represses IGF-1R expression and inhibits IGF-1R signaling

To evaluate the role of NRP2 in prostate tumorigenesis, we generated PC3 cells with diminished NRP2 expression using shRNAs. Loss of NRP2 had no effect on morphology or proliferation on tissue culture plates (data not shown), but it did reduce the ability of these cells to grow in soft agar (Fig. 4A, left). The NRP2-depleted cells also grew more slowly compared to control cells when implanted subcutaneously in mice (Fig. 4A, right). Although significant, the impact of NRP2 loss on growth in soft agar and tumor formation *in vivo* was modest suggesting a potential compensatory mechanism. In this context, we observed a marked increase in IGF-1R mRNA expression concomitant with NRP2 loss but no change in

the expression of either EGFR or insulin receptor mRNA expression (Fig. 4B). This effect of NRP2 loss on the induction of IGF-1R expression was also evident at the protein level in both PC3 and C4-2 cells (Fig. 4C). This effect is specific to NRP2 because no change in IGF-1R expression was observed upon NRP1 loss (Fig. 4D). The repression of IGF-1R expression by NRP2 in PC3 cells was maintained *in vivo* as evidenced by the observation that loss of NRP2 induced a significant increase in IGF-1R in three independent xenograft tumors (Fig. 4E). Also, immunostaining of human prostate cancer specimens revealed a positive correlation between p-AKT and NRP2 expression, but a negative correlation between NRP2 and IGF-1R (Supplementary Fig. 3B-C). The possibility existed that FOXO transcription factors contribute to the regulation of IGF-1R expression based on the recent report that PI3K activation represses receptor tyrosine kinases including the IGF1R by feedback inhibition through inactivation of FOXO transcription factors (32). However, no change in FOXO activation was observed upon NRP2 depletion and down-regulation of FOXO factors did not affect the induction of IGF-1R expression caused by NRP2 (Supplementary Fig. 5A-C). Thus, the mechanism we propose appears to be distinct from this interesting study because inactivation of FOXO factors affected a number of receptors including the insulin receptor, EGFR and c-met. In contrast, NRP2 represses only the IGF-1R (Fig. 4B).

To investigate the role of NRP2 on IGF-1R signaling and function further, we expressed NRP2 in non-cancerous prostate epithelial cells p69, which express high levels of IGF-1R and less c-Jun compared to more aggressive cell lines (33). p69 cells are NRP2-null and expression of NRP2 reduced IGF-1R levels (Fig. 4F). These cells also express endogenous VEGF (Supplementary Fig. 5D). Consistent with reduced IGF-1R expression, NRP2 expression inhibited IGF-1 stimulated cell proliferation (Fig. 4G, left) and IRS-1 phosphorylation (a substrate of IGF-1R tyrosine kinase) (Fig. 4G, right). Based on these results, it is expected that PTEN positive tumors, which express low levels of NRP2, have high IGF-1R levels. This hypothesis was confirmed by analyzing gene expression derived from human prostate cancer specimens (n=128) (34). We found a positive correlation between IGF-1R and PTEN expression ($p=2\times10^{-5}$) (Fig. 4H).

The compensatory relationship between NRP2 and IGF-1R expression indicated that inhibition of both receptors would be more effective at impeding tumor growth than inhibition of either receptor individually. To test this hypothesis, we investigated the effect of an IGF-1R inhibitory antibody on the ability of control PC3 cells or cells in which NRP2 expression had been ablated to grow in soft agar or in immunocompromised mice. A significant effect of combined NRP2 down-regulation and IGF-1R inhibition was evident in both soft agar growth *in vitro* (Fig. 4I) and tumor growth *in vivo* (Fig. 4J) ($p<0.01$). Indeed, combined treatment resulted in complete inhibition of tumor growth (Fig. 4J). The inhibition of NRP2 and IGF-1R did not change the expression of the insulin receptor (Supplementary Fig. 6A), discounting the possibility of compensation by this receptor. Moreover, combined treatment significantly increased the cleavage of caspase 3, suggesting activation of cell death pathway (Supplementary Fig. 6B). Addition of A12 blocked IGF-1 stimulated tyrosine phosphorylation of IRS-1, validating the functionality of this antibody (Supplementary Fig. 6C). Further evidence in support of our findings was provided by the effect of A12 on PTEN-null (PC3) and PTEN-postitive (VCaP) prostate cancer cell lines. In agreement with

our hypothesis, A12 inhibited cell proliferation of VCaP, but not PC3 cells (Supplementary Fig. 6D).

VEGF/NRP2 signaling regulates Bmi-1, which represses IGF-1R transcription

To establish the mechanism by which NRP2 represses the IGF-1R, we focused on our novel finding that NRP2 is required to maintain expression of Bmi-1, a Polycomb group transcriptional repressor that has been implicated in PTEN-deletion-induced prostate cancer (16). Specifically, NRP2 loss in both PC3 and C4-2 cells diminished Bmi-1 protein expression markedly (Fig. 5A), as well as Bmi-1 mRNA expression in PC3 cells (Fig. 5B, left). This effect of NRP2 loss on Bmi-1 expression was also observed in PC3 xenografts (Fig. 5B, right). These data linking NRP2 to Bmi-1 imply that NRP2 has a role in tumor formation. This effect was manifested in soft agar assays because over-expression of Bmi-1 rescued soft agar growth caused by NRP2 down-regulation (Fig. 5C). Moreover, analysis of the gene expression data from Taylor et al. (34), revealed a positive correlation between expression of Bmi-1 and c-Jun ($p=1 \times 10^{-6}$) (Fig. 5D).

Given that Bmi-1 is a transcriptional repressor and our finding that NRP2 represses expression of the IGF-1R, we examined the ability of Bmi-1 to repress IGF-1R transcription. Initially, we observed that depletion of Bmi-1 expression in PC3 cells using shRNAs increased IGF-1R mRNA levels (Fig. 5E). Loss of Bmi-1 also increased expression of the IGF-1R protein significantly confirming the importance of Bmi-1 in repressing IGF-1R expression (Fig. 5F). To investigate the regulation of IGF-1R by Bmi-1, we performed ChIP using a Bmi-1 Ab and discovered that Bmi-1 binds directly to the IGF-1R promoter (Fig. 5G). More specifically, Bmi-1 appears to bind to a region between −74 and −756 in the promoter (Fig. 5G). As further proof that NRP2 represses IGF-1R expression by a Bmi-1-dependent mechanism, we infected PC3 cells that had been depleted of NRP2 with a lentivirus expressing Bmi-1 and assessed IGF-1R expression. We observed that Bmi-1 represses IGF-1R expression in the absence of NRP2 (Fig. 5H).

Recently, we reported that VEGF/NRP2 signaling activates focal adhesion kinase (FAK) in concert with the α6β1 integrin (35, 36), and we observed that NRP2 and α6β1 interact in prostate carcinoma cells (Supplementary Fig. 6E). To investigate whether NRP2 mediated Bmi-1 expression involves FAK signaling, we evaluated FAK activation in tumor samples *in vivo*. Tumor xenografts from NRP2-depleted cells show reduced FAK activation (Fig. 6A) and treatment of PC3 cells with a FAK inhibitor reduced expression of Bmi-1 (Fig. 6B). In addition, we also assessed FAK activation in tumor samples by immunostaining. We found that NRP2-high (PTEN-low) tumors express high levels of activated FAK (also localized to membrane) compared to NRP2-low (PTEN positive) tumors (Fig. 6C). These data were confirmed by over-expression of constitutively active FAK (K38A) in NRP2-depleted cells, which resulted in increased expression of Bmi-1 (Fig. 6D). To analyze the effect of c-Jun expression on FAK activation, we used LNCaP cells expressing low levels of NRP2 and observed that c-Jun expression increases NRP2, as well as FAK activation (Fig. 6E). Similarly, downregulation of c-Jun reduced FAK activation and Bmi-1 expression; however, increased IGF-1R levels (Fig. 6F).

A critical issue is whether the observed effects of NRP2 on Bmi-1 and IGF-1R expression involve VEGF, a NRP2 ligand. To address this issue, we down-regulated VEGF expression in PC3 cells using either siRNA or shRNA, and observed that decreased VEGF expression is associated with decreased Bmi-1 and increased IGF-1R expression (Fig. 7A-B, Supplementary Fig. 6F). Moreover, exogenous VEGF increased Bmi-1 expression in a dose-dependent manner (Supplementary Fig. 6G). Our data also imply that VEGF expression should be higher in prostate tumors with PTEN loss compared with PTEN-positive tumors and that it should correlate with NRP2 and inversely with IGF-1R expression. To assess this hypothesis, qPCR was performed using RNA isolated from 12 prostate tumors (6 $PTEN^{low}$ and 6 $PTEN^{high}$). The $PTEN^{low}$ tumors exhibited relatively high expression of NRP2 and VEGF but low expression of the IGF-1R compared to the $PTEN^{high}$ tumors (Fig. 7C). The expression pattern of VEGF is consistent with our finding that VEGF expression in tumor cells correlates with Gleason grade (20). To exclude the possibility that VEGF regulation of Bmi-1 is mediated by other VEGF receptors, especially VEGF tyrosine kinase receptors, we used bevacizumab, which inhibits the interaction of VEGF with these receptors but not with NRP2 (22). A NRP2-blocking Ab inhibited VEGF induction of Bmi-1 expression but bevacizumab had no significant effect (Fig. 7D).

NRP2 is a biomarker that predicts response to IGF-1R therapy

Collectively, the data generated in this study indicate that NRP2 expression in tumor cells is a potential biomarker to predict the efficacy of IGF-1R inhibitors, which are currently in clinical trials. To test this latter possibility, we used two LuCaP xenograft models: LuCaP-35 and LuCaP-86.2. LuCaP-35 is sensitive to the IGF-1R inhibitor A12 and tumor growth is substantially inhibited upon A12 treatment. In contrast, LuCaP-86.2 is insensitive to A12 (Fig. 7E). We detected significantly reduced expression of IGF-1R and increased expression of NRP2 and Bmi-1 in LuCaP-86.2 (PTEN-null) compared to LuCaP-35 (PTEN +) tumors. Conversely, LuCaP-35 tumors expressed significantly higher levels of IGF-1R compared to NRP2 and Bmi-1 (Fig. 7F). These data were further strengthened by the analysis of an additional 15 A12-responders and 8 A12 non-responders (Fig. 7G, Supplementary Fig. 7). As shown in Fig. 7G, we detected 150-fold more NRP2 expression in the non-responders compared to responders and only a 10-fold increase in IGF-1R expression in the responders compared to the non-responders. To further substantiate our finding that NRP2 loss can enhance sensitivity to IGF-1R inhibition, we ablated NRP2 expression in LuCaP 86.2 cells and observed a significant increase in the response to A12 as assessed by cell proliferation (Fig. 7H). Importantly, this response is associated with a significant decrease in Bmi-1 expression and increase in IGF-1R expression (Fig. 7H).

DISCUSSION

Our data highlight a novel role for VEGF/NRP2 signaling in prostate cancer cells that impacts our understanding of the biological nature of this disease, especially aggressive prostate cancer, and our approach to therapy. Specifically, we conclude that the VEGF receptor NRP2 is induced by PTEN loss and that VEGF/NRP2 signaling regulates the expression of Bmi-1, a key effector of prostate tumorigenesis induced by PTEN deletion (16). The consequences of this mechanism are significant for several reasons, including our

finding that Bmi-1 represses transcription of the IGF-1R and abrogates IGF-1R signaling. We exploited these results to demonstrate that NRP2 is a novel biomarker for high-grade prostate cancer that can be used to predict response to IGF-1R therapy. Importantly, our work indicates that combined NRP2 and IGF-1R inhibition is an effective approach for impeding tumor growth that overcomes the resistance caused by inhibiting either receptor independently.

A major conclusion from our work is that NRP2 expression and function are linked directly to oncogenic transformation associated with loss of PTEN function. More specifically, we show that PTEN loss induces NRP2 expression by activating JNK1/c-Jun and that an inverse correlation between PTEN and NRP2 expression is evident in both the $PTEN^{pc-/-}$ mice and in human prostate cancer. These expression data were substantiated by our finding that VEGF/NRP2 signaling regulates the expression of Bmi-1, a Polycomb group transcriptional repressor implicated in prostate tumorigenesis (16). Although a previous study had foreshadowed a role for NRP2 in the xenograft growth of colorectal carcinoma cells (37), our study is the first to demonstrate that an oncogenic pathway, i.e., c-Jun activation induced by PTEN loss, regulates NRP2. Moreover, our finding that NRP2 expression increases with Gleason grade is consistent with our previous finding that VEGF expression in cancer cells also increases with Gleason grade (20), supporting the hypothesis that autocrine VEGF/NRP2 signaling is characteristic of high-grade, aggressive prostate cancer. We do not exclude the possibility that this signaling pathway involves other VEGF receptors in addition to NRP2. Specifically, prostate carcinoma cells express VEGFR2 but lack expression of VEGFR1 (Supplementary Fig. 2E). The absence of VEGFR1 is consistent with previous reports and may result from hypermethylation of the VEGFR1 gene in prostate cancer (23, 24). Nonetheless, the possibility that VEGFR2 contributes to NRP2 signaling is mitigated but not discounted by our finding that bevacizumab, which inhibits the interaction of VEGF with tyrosine kinase VEGF receptors but not with NRP2 (22), did not inhibit the ability of VEGF to regulate Bmi-1

Unexpectedly, we identified NRP2 as a novel c-Jun target that is regulated by PTEN. The implication of these findings is that VEGF/NRP2 signaling is a component of the mechanism by which PTEN loss induces prostate cancer. Our key findings that VEGF/NRP2 signaling regulates Bmi-1 expression and that there is a strong correlation between NRP2 and Bmi-1 in human prostate cancer buttress this conclusion. The significance of these data is that they provide a causal link between VEGF/NRP2 signaling and a mechanism of prostate tumorigenesis, and they build upon the seminal report that Bmi-1 regulates the self-renewal of prostate stem cells and malignant transformation (16). Our data provide a specific mechanism (autocrine VEGF/NRP2 signaling) that contributes to Bmi-1 regulation in prostate cancer. Of note, this mechanism is consistent with the hypothesis that tumor stem cells secrete growth factors in an autocrine manner to protect themselves from differentiation and to support their self-renewal (38).

An important issue that arises from our data is how VEGF signals through NRP2 given that NRP2 lacks intrinsic signaling function. We hypothesize that the specific interaction between NRP2 and the $\alpha 6\beta 1$ integrin (CD49f) potentiates this signaling. This hypothesis is based on our previous finding that NRP2 facilitates the $\alpha 6\beta 1$-mediated activation of FAK

and Src (36) and our observation here that NRP2 and α6β1 interact in prostate carcinoma cells. Interestingly the association of NRP2 with α6β1 does not require the cytoplasmic domain of NRP2 (Supplementary Fig. 6E) indicating that this association occurs in the membrane, perhaps in microdomains enriched for these receptors. We stress that our findings do not discount a role for tyrosine kinase VEGF receptors in promoting NRP2 signaling. Numerous studies have shown that the NRPs can enhance the function of these receptors (6, 7). It is important to note, however, that even if such VEGF receptors contribute to the signaling pathway we describe, NRP2 is essential and a prime target for therapeutic intervention. Moreover, the data presented in Fig. 4J indicate that targeting NRP2 and IGF-1R is sufficient to block tumor growth in the absence of any other VEGF receptor inhibition.

We implicate FAK as a downstream effector of VEGF/NRP2 signaling that regulates Bmi-1 expression. This ability of FAK to regulate Bmi-1 is novel and it adds to our understanding of how FAK contributes to tumorigenesis. FAK expression is increased in prostate cancer cells compared to prostatic epithelium, and there is evidence that FAK participates in prostate tumorogenesis (39). FAK is also necessary for mammary tumorigenesis and for the function of mammary tumor stem cells (40) but the mechanism by which FAK functions in this capacity has not been elucidated. Clearly, the ability of FAK to regulate Bmi-1 provides one such mechanism. As mentioned above, it is likely that the α6β1 integrin is a component of this mechanism (35, 36).

Our data support the conclusion that IGF-1R expression and signaling are diminished in high-grade, aggressive prostate cancer, most likely as a result of PTEN loss. Although this conclusion is unexpected because IGF-1R signaling is thought to promote tumor proliferation in prostate and other cancers (41), this receptor can also promote differentiation (42, 43) and this function may need to be impeded by VEGF/NRP2 signaling for the genesis of high-grade, aggressive cancer. This possibility is supported by the report that abrogation of functional IGF-IR expression actually promoted earlier emergence of more aggressive, less-differentiated carcinomas in a p53-compromised model of prostate cancer (44).

The data presented have significant implications for the prostate cancer therapy, especially because the clinical use of IGF-IR inhibitors is feasible (17) and NRP2 inhibitors are available (13). Based on our data, most of the ongoing IGF-1R clinical trials will not succeed because these trials recruited many patients with high-grade, aggressive prostate cancer, which expresses NRP2 but lacks IGF-1R and PTEN expression. Inhibition of the IGF-1R may reduce the burden of low-grade tumors but such tumors likely contain a small population of $NRP2^{+}$ cells that are resistant to IGF-1R inhibition and will cause relapse unless this VEGF receptor is also targeted. NRP2 inhibition could be a very effective therapy for aggressive, high-grade tumors provided that the IGF-1R is also inhibited to reduce tumor burden caused by compensatory signaling. In summary, this study identifies NRP2 as a novel biomarker for predicting response to IGF-1R therapy. A critical finding in this context is that NRP2 is a much more robust biomarker than the IGF-1R itself. This finding is significant because the IGF-1R, is also expressed normal glands, in contrast to NRP2. Importantly, the data presented provide a rationale for initiating clinical trials that combine inhibitors of both NRP2 and IGF-1R.

METHODS

Clinical specimens

Tissue samples of defined Gleason grade, lymph node and bone metastases were obtained from the UMASS Cancer Center Tissue Bank with approval of the Institutional Review Board (IRB) of UMASS Medical School. The IRB granted a waiver for obtaining patients consent in accordance with National Institute of Health guidelines because these are pre-existing, de-identified specimens. Formain-fixed paraffin-embedded sections either from primary tumors, lymph node metastases or bone metastases were stained using either NRP2 or control IgG Ab as described before (20). Frozen sections were microdissected by laser capture microscopy (Arcturus PixCell 2) as described elsewhere (20) to obtain pure populations of tumor cells of defined Gleason grades. RNA was isolated from these microdissected samples using the RNeasy kit (Qiagen) and prepared cDNA using Superscript II reverse transcriptase (invitrogen). Quantitative real-time PCR was done using the Taqman assay kit (Apllied Biosystems): PTEN (Hs02621230_s1), NRP2 (Hs00187290_m1), VEGF (Hs00900055_m1), IGF-1R (Hs00609566_m1), GAPDH (Hs9999905_m1). Tissue microarrays containing 52 primary prostate cancer tissues were also used.

Reagents and antibodies

Bmi-1 (Cell Signaling), Actin (Sigma), IGF-1R (Cell signaling), NRP2 (C-9, H-300, Santa Cruz and R&D), p-FAK (Y397, Invitrogen) a-VEGF (Calbiocehm), insulin receptor (SantaCruz), cleaved caspase 3, PTEN (Cell Signaling), p-Tyr (PY99), NRP1 (Santa Cruz), pAKT (Ser473), pS6K, pFOXO1 (Ser256), FOXO1 (L27), AKT, S6K, p-c-Jun (S73, Cell Signaling), c-Jun (Santa Cruz), IRS-1 (Bethyl) and CD49f (AA6A; kindly provided by Dr. A. Cress). Bevacizumab was obtained from the pharmacy of UMass Memorial Medical Center. A12, Cixutumumab, was kindly supplied by Dr. Dale Ludwig from ImClone Systems Incorporated, Branchburg, New Jersey. IHC for pAKT was performed using D9E Ab (Cell signaling). IGF-1R Ab, α-IR3 was purchased from Abcam. PF573228 (FAK inhibitor) is from Tocris.

Constructs—The PTEN plasmid was provided by Dr. Alonzo Ross (UMASS Medical School); Bmi-1-ires-eGFP cloned into FUGW was obtained from Addgene; c-Jun expression constructs (HA-tagged) were provided by Dr. Dirk Bohmann (University of Rochester Medical Center); CA-FAK (K38A) construct was provided by Jun-Lin Guan (University of Michigan). Lentiviruses vectors expressing NRP2 shRNAs (Open Biosystems, Huntsville, AL, USA; clone ID TRCN0000063308, TRCN0000063309 or TRCN0000063312), VEGF shRNA (TRCN0000003343), Bmi-1 shRNA (TRCN0000020154, TRCN0000020156, TRCN0000012565) or c-Jun shRNAs (provided by S. Huang, Georgia Health Sciences University) or a GFP control (Open Biosystems, RHS4459) were used.

Cells and transfectants

Prostate cancer cells, LNCaP, PC3, VCaP, DU145 (ATCC), C4-2 (UroCor, Inc.) or normal prostate immortalized cell lines RWPE-1 (provided by Dr. SK Batra, UNMC, Nebraska),

PNT1A (provided by Dr. M. Ittmann, Baylor College of Medicine), PZ-HPV7 (provided by Dr. TC Chen, BU, Boston, MA) were used. PC3-M cells (45) were kindly provided by Dr. Paul Mak (UMASS Medical School). These cell lines were not authenticated. Lentiviruses containing NRP2 shRNAs, VEGF shRNA, Bmi-1 shRNA or c-Jun shRNAs or a GFP control were generated, titrated according to the manufacturer's instructions and used to infect cells following standard protocols. Stable cell transfectants were generated by puromycin selection (2 mg/ml). In some experiments, cells were transfected with VEGF siRNA (Smartpool, Dharmacon, Lafayette, CO, USA) or scrambled control siRNA.

Anchorage-independent growth assays

Growth in soft agar was assayed by scoring the number of colonies formed in medium (DMEM supplemented with 10% FBS) containing 0.3% agarose, with a 0.5% agarose medium underlay as described (46). PC3-parental, PC3-GFP-sh or PC3-NRP2-sh (NRP2-sh-1 or NRP2-sh-2) cells were seeded on 60-mm diameter plates in triplicate. Cells were fed with 1.5 mL of suspension medium (DMEM supplemented with 10% FBS) every 3 days. The number of colonies larger than 100 μm was counted after 14 days.

$Pten^{pc-/-}$ mice

The *Pten*$^{pc-/-}$ mice (26), backcrossed more than 10 times to obtain a Balb/c background. Specimens of PIN (6 wks) or invasive prostate tumors (20 wks) from these mice and mice with wild-type PTEN were stained for NRP2 or NRP1 expression using IHC.

Luciferase assays

Cells were transfected with the luciferase construct and Renilla luciferase construct to normalize for transfection efficiency. Relative light units were calculated as the ratio of firefly luciferase to Renilla luciferase activity (normalized luciferase activity). The protocol used for transfection and measurement of luciferase activity has been described previously (20). We used a NRP2 promoter luciferase construct (−3000/+195) or the same construct with AP1 mutations. A full-length wild-type c-jun promoter (−1780/+731) luciferase construct was provided by Dr. Wayne Vedeckis (LSU Health Sciences Center) and used to study the effect of PTEN expression.

ChIP assays

ChIP assays were performed according to our published protocol (47). All ChIP experiments were performed at least thrice and the variation was less than 20%. The primers used to amplify the IGF-1R and NRP2 promoters, as well as other genes analyzed in this study, are provided in Supplementary Fig. 8.

Xenografts

Tumor fragments (20-30 mm^3) from the human prostate tumor xenografts (LuCaP 35 or LuCap-86.2; established by co-author RLV) were implanted s.c. into 6-week-old castrated severe combined immunodeficient mice as previously described (48, 49). Once the implanted tumor was reached a volume of ~100 mm^3, animals were randomized into two groups (10 mice per group). Group 1 animals received human IgG treatment and were

designated as controls. Group 2 animals received A12 treatment at a dose of 40 mg/kg. All treatments were given i.p. thrice a week for 4 weeks. Tumors were measured twice weekly and tumor volume was estimated by the formula: volume = $L \times W^2/2$. Single-cell suspensions of LuCaP 86.2 cells were prepared by resecting the s.c. xenografts and cutting them into small pieces in DMEM/F12 containing 10% FBS. The small pieces were mechanically dissociated and cell viability was determined by trypan blue counting as described (50). Cells were cultured in DMEM/F12 containing 20% FBS and 5 ng/ml EGF. PC3 transfectants (sh-GFP, or sh-NRP2) implanted in immuno-compromised mice were injected i.p. with either A12 or IgG, once the tumor volume reached ~150mm^3. Xenograft growth was measured on alternate days.

Cell-based assays

Cell proliferation was measured using MTT assay. Cell invasion assays were performed using Matrigel-coated transwell plates.

Supplementary Material

Refer to Web version on PubMed Central for supplementary material.

Acknowledgments

We thank Drs. S. K. Batra, Azad Bonni, T. C. Chen, M. Ittmann, A. Ross, L. Shaw, V. Sharma, C. Cheng and P. Mak for reagents, cell lines, technical assistance and manuscript discussion. We also thank Michael Roche and Dr. Cherie Taglienti from UMass Tissue Bank for their help with human tissue specimens.

Grant Support

This work was supported by NIH Grants R01CA80789 and CA89209 (A.M.M.); R01CA59705 (P.R-B.); PO1 CA85859 and the Pacific Northwest Prostate Cancer SPORE P50 CA097186 (S.R.P., R.L.V. and P.S.N.); the Veterans Affairs Research Program (S.R.P.) and an award from the Prostate Cancer Foundation (P.S.N).

References

1. Siegel R, Ward E, Brawley O, Jemal A. Cancer statistics, 2011: The impact of eliminating socioeconomic and racial disparities on premature cancer deaths. CA Cancer J Clin. 2011; 61:212–36. [PubMed: 21685461]
2. Bachelder RE, Crago A, Chung J, Wendt MA, Shaw LM, Robinson G, et al. Vascular endothelial growth factor is an autocrine survival factor for neuropilin-expressing breast carcinoma cells. Cancer Res. 2001; 61:5736–40. [PubMed: 11479209]
3. Lichtenberger BM, Tan PK, Niederleithner H, Ferrara N, Petzelbauer P, Sibilia M. Autocrine VEGF signaling synergizes with EGFR in tumor cells to promote epithelial cancer development. Cell. 2010; 140:268–79. [PubMed: 20141840]
4. Muders MH, Zhang H, Wang E, Tindall DJ, Datta K. Vascular endothelial growth factor-C protects prostate cancer cells from oxidative stress by the activation of mammalian target of rapamycin complex-2 and AKT-1. Cancer Res. 2009; 69:6042–8. [PubMed: 19638584]
5. Beck B, Driessens G, Goossens S, Youssef KK, Kuchnio A, Caauwe A, et al. A vascular niche and a VEGF-Nrp1 loop regulate the initiation and stemness of skin tumours. Nature. 2011; 478:399–403. [PubMed: 22012397]
6. Bagri A, Tessier-Lavigne M, Watts RJ. Neuropilins in tumor biology. Clin Cancer Res. 2009; 15:1860–4. [PubMed: 19240167]
7. Klagsbrun M, Takashima S, Mamluk R. The role of neuropilin in vascular and tumor biology. Adv Exp Med Biol. 2002; 515:33–48. [PubMed: 12613541]

8. Soker S, Takashima S, Miao HQ, Neufeld G, Klagsbrun M. Neuropilin-1 is expressed by endothelial and tumor cells as an isoform-specific receptor for vascular endothelial growth factor. Cell. 1998; 92:735–45. [PubMed: 9529250]

9. Neufeld G, Kessler O, Herzog Y. The interaction of Neuropilin-1 and Neuropilin-2 with tyrosine-kinase receptors for VEGF. Adv Exp Med Biol. 2002; 515:81–90. [PubMed: 12613545]

10. Sulpice E, Plouet J, Berge M, Allanic D, Tobelem G, Merkulova-Rainon T. Neuropilin-1 and neuropilin-2 act as coreceptors, potentiating proangiogenic activity. Blood. 2008; 111:2036–45. [PubMed: 18065694]

11. Gray MJ, Wey JS, Belcheva A, McCarty MF, Trevino JG, Evans DB, et al. Neuropilin-1 suppresses tumorigenic properties in a human pancreatic adenocarcinoma cell line lacking neuropilin-1 coreceptors. Cancer Res. 2005; 65:3664–70. [PubMed: 15867361]

12. Gray MJ, Van Buren G, Dallas NA, Xia L, Wang X, Yang AD, et al. Therapeutic targeting of neuropilin-2 on colorectal carcinoma cells implanted in the murine liver. J Natl Cancer Inst. 2008; 100:109–20. [PubMed: 18182619]

13. Caunt M, Mak J, Liang WC, Stawicki S, Pan Q, Tong RK, et al. Blocking neuropilin-2 function inhibits tumor cell metastasis. Cancer Cell. 2008; 13:331–42. [PubMed: 18394556]

14. Pan Q, Chanthery Y, Liang WC, Stawicki S, Mak J, Rathore N, et al. Blocking neuropilin-1 function has an additive effect with anti-VEGF to inhibit tumor growth. Cancer Cell. 2007; 11:53–67. [PubMed: 17222790]

15. McMenamin ME, Soung P, Perera S, Kaplan I, Loda M, Sellers WR. Loss of PTEN expression in paraffin-embedded primary prostate cancer correlates with high Gleason score and advanced stage. Cancer Res. 1999; 59:4291–6. [PubMed: 10485474]

16. Lukacs RU, Memarzadeh S, Wu H, Witte ON. Bmi-1 is a crucial regulator of prostate stem cell self-renewal and malignant transformation. Cell Stem Cell. 2010; 7:682–93. [PubMed: 21112563]

17. Gualberto A, Pollak M. Emerging role of insulin-like growth factor receptor inhibitors in oncology: early clinical trial results and future directions. Oncogene. 2009; 28:3009–21. [PubMed: 19581933]

18. Pollak M. The insulin receptor/insulin-like growth factor receptor family as a therapeutic target in oncology. Clin Cancer Res. 2012; 18:40–50. [PubMed: 22215905]

19. Kwak C, Jin RJ, Lee C, Park MS, Lee SE. Thrombospondin-1, vascular endothelial growth factor expression and their relationship with p53 status in prostate cancer and benign prostatic hyperplasia. BJU Int. 2002; 89:303–9. [PubMed: 11856116]

20. Mak P, Leav I, Pursell B, Bae D, Yang X, Taglienti CA, et al. ERbeta impedes prostate cancer EMT by destabilizing HIF-1alpha and inhibiting VEGF-mediated snail nuclear localization: implications for Gleason grading. Cancer Cell. 2010; 17:319–32. [PubMed: 20385358]

21. Reese DM, Fratesi P, Corry M, Novotny W, Holmgren E, Small EJ. A Phase II Trial of Humanized Anti-Vascular Endothelial Growth Factor Antibody for the Treatment of Androgen-Independent Prostate Cancer. The Prostate Journal. 2001; 3:65–70.

22. Geretti E, van Meeteren LA, Shimizu A, Dudley AC, Claesson-Welsh L, Klagsbrun M. A mutated soluble neuropilin-2 B domain antagonizes vascular endothelial growth factor bioactivity and inhibits tumor progression. Mol Cancer Res. 2010; 8:1063–73. [PubMed: 20651020]

23. Hahn D, Simak R, Steiner GE, Handisurya A, Susani M, Marberger M. Expression of the VEGF-receptor Flt-1 in benign, premalignant and malignant prostate tissues. J Urol. 2000; 164:506–10. [PubMed: 10893635]

24. Yamada Y, Watanabe M, Yamanaka M, Hirokawa Y, Suzuki H, Takagi A, et al. Aberrant methylation of the vascular endothelial growth factor receptor-1 gene in prostate cancer. Cancer Sci. 2003; 94:536–9. [PubMed: 12824880]

25. Schmitz M, Grignard G, Margue C, Dippel W, Capesius C, Mossong J, et al. Complete loss of PTEN expression as a possible early prognostic marker for prostate cancer metastasis. Int J Cancer. 2007; 120:1284–92. [PubMed: 17163422]

26. Wang S, Gao J, Lei Q, Rozengurt N, Pritchard C, Jiao J, et al. Prostate-specific deletion of the murine Pten tumor suppressor gene leads to metastatic prostate cancer. Cancer Cell. 2003; 4:209–21. [PubMed: 14522255]

27. Majumder PK, Sellers WR. Akt-regulated pathways in prostate cancer. Oncogene. 2005; 24:7465–74. [PubMed: 16288293]
28. Vivanco I, Palaskas N, Tran C, Finn SP, Getz G, Kennedy NJ, et al. Identification of the JNK signaling pathway as a functional target of the tumor suppressor PTEN. Cancer Cell. 2007; 11:555–69. [PubMed: 17560336]
29. Mulholland DJ, Tran LM, Li Y, Cai H, Morim A, Wang S, et al. Cell autonomous role of PTEN in regulating castration-resistant prostate cancer growth. Cancer Cell. 2011; 19:792–804. [PubMed: 21620777]
30. Lin FJ, Chen X, Qin J, Hong YK, Tsai MJ, Tsai SY. Direct transcriptional regulation of neuropilin-2 by COUP-TFII modulates multiple steps in murine lymphatic vessel development. J Clin Invest. 2010; 120:1694–707. [PubMed: 20364082]
31. Weston CR, Davis RJ. The JNK signal transduction pathway. Curr Opin Cell Biol. 2007; 19:142–9. [PubMed: 17303404]
32. Chandarlapaty S, Sawai A, Scaltriti M, Rodrik-Outmezguine V, Grbovic-Huezo O, Serra V, et al. AKT inhibition relieves feedback suppression of receptor tyrosine kinase expression and activity. Cancer Cell. 2011; 19:58–71. [PubMed: 21215704]
33. Plymate SR, Tennant M, Birnbaum RS, Thrasher JB, Chatta G, Ware JL. The effect on the insulin-like growth factor system in human prostate epithelial cells of immortalization and transformation by simian virus-40 T antigen. J Clin Endocrinol Metab. 1996; 81:3709–16. [PubMed: 8855827]
34. Taylor BS, Schultz N, Hieronymus H, Gopalan A, Xiao Y, Carver BS, et al. Integrative genomic profiling of human prostate cancer. Cancer Cell. 2010; 18:11–22. [PubMed: 20579941]
35. Goel HL, Bae D, Pursell B, Gouvin LM, Lu S, Mercurio AM. Neuropilin-2 promotes branching morphogenesis in the mouse mammary gland. Development. 2011; 138:2969–76. [PubMed: 21693513]
36. Goel HL, Pursell B, Standley C, Fogarty K, Mercurio AM. Neuropilin-2 Regulates the Ability of the α6β1 Integrin to Form Focal Adhesions and Signal. J Cell Sci. 2012; 125:497–506. [PubMed: 22302985]
37. Grandclement C, Pallandre JR, Valmary Degano S, Viel E, Bouard A, Balland J, et al. Neuropilin-2 expression promotes TGF-beta1-mediated epithelial to mesenchymal transition in colorectal cancer cells. PLoS One. 2011; 6:e20444. [PubMed: 21747928]
38. Scheel C, Eaton EN, Li SH, Chaffer CL, Reinhardt F, Kah KJ, et al. Paracrine and autocrine signals induce and maintain mesenchymal and stem cell states in the breast. Cell. 2011; 145:926–40. [PubMed: 21663795]
39. Slack-Davis JK, Hershey ED, Theodorescu D, Frierson HF, Parsons JT. Differential requirement for focal adhesion kinase signaling in cancer progression in the transgenic adenocarcinoma of mouse prostate model. Mol Cancer Ther. 2009; 8:2470–7. [PubMed: 19671741]
40. Luo M, Fan H, Nagy T, Wei H, Wang C, Liu S, et al. Mammary epithelial-specific ablation of the focal adhesion kinase suppresses mammary tumorigenesis by affecting mammary cancer stem/progenitor cells. Cancer Res. 2009; 69:466–74. [PubMed: 19147559]
41. Sell C, Rubini M, Rubin R, Liu JP, Efstratiadis A, Baserga R. Simian virus 40 large tumor antigen is unable to transform mouse embryonic fibroblasts lacking type 1 insulinlike growth factor receptor. Proc Natl Acad Sci U S A. 1993; 90:11217–21. [PubMed: 8248231]
42. Massoner P, Ladurner Rennau M, Heidegger I, Kloss-Brandstatter A, Summerer M, Reichhart E, et al. Expression of the IGF axis is decreased in local prostate cancer but enhanced after benign prostate epithelial differentiation and TGF-beta treatment. Am J Pathol. 2011; 179:2905–19. [PubMed: 21983635]
43. Valentinis B, Romano G, Peruzzi F, Morrione A, Prisco M, Soddu S, et al. Growth and differentiation signals by the insulin-like growth factor 1 receptor in hemopoietic cells are mediated through different pathways. J Biol Chem. 1999; 274:12423–30. [PubMed: 10212216]
44. Sutherland BW, Knoblaugh SE, Kaplan-Lefko PJ, Wang F, Holzenberger M, Greenberg NM. Conditional deletion of insulin-like growth factor-I receptor in prostate epithelium. Cancer Res. 2008; 68:3495–504. [PubMed: 18451178]

45. Pettaway CA, Pathak S, Greene G, Ramirez E, Wilson MR, Killion JJ, et al. Selection of highly metastatic variants of different human prostatic carcinomas using orthotopic implantation in nude mice. Clin Cancer Res. 1996; 2:1627–36. [PubMed: 9816342]

46. Goel HL, Breen M, Zhang J, Das I, Aznavoorian-Cheshire S, Greenberg NM, et al. beta1A integrin expression is required for type 1 insulin-like growth factor receptor mitogenic and transforming activities and localization to focal contacts. Cancer Res. 2005; 65:6692–700. [PubMed: 16061650]

47. Yang X, Pursell B, Lu S, Chang TK, Mercurio AM. Regulation of beta 4-integrin expression by epigenetic modifications in the mammary gland and during the epithelial-tomesenchymal transition. J Cell Sci. 2009; 122:2473–80. [PubMed: 19549682]

48. Wu JD, Odman A, Higgins LM, Haugk K, Vessella R, Ludwig DL, et al. In vivo effects of the human type I insulin-like growth factor receptor antibody A12 on androgen-dependent and androgen-independent xenograft human prostate tumors. Clin Cancer Res. 2005; 11:3065–74. [PubMed: 15837762]

49. Sun S, Sprenger CC, Vessella RL, Haugk K, Soriano K, Mostaghel EA, et al. Castration resistance in human prostate cancer is conferred by a frequently occurring androgen receptor splice variant. J Clin Invest. 2010; 120:2715–30. [PubMed: 20644256]

50. Zhang J, Dai J, Yao Z, Lu Y, Dougall W, Keller ET. Soluble receptor activator of nuclear factor kappaB Fc diminishes prostate cancer progression in bone. Cancer Res. 2003; 63:7883–90. [PubMed: 14633717]

SIGNIFICANCE

These results identify a causal role for NRP2 and VEGF/NRP2 signaling in the behavior of aggressive prostate cancers by a mechanism that involves regulation of Bmi-1, a transcriptional repressor implicated in the etiology of prostate cancer induced by loss of PTEN function, and the repression of the IGF-1R. The therapeutic implications of these data are significant.

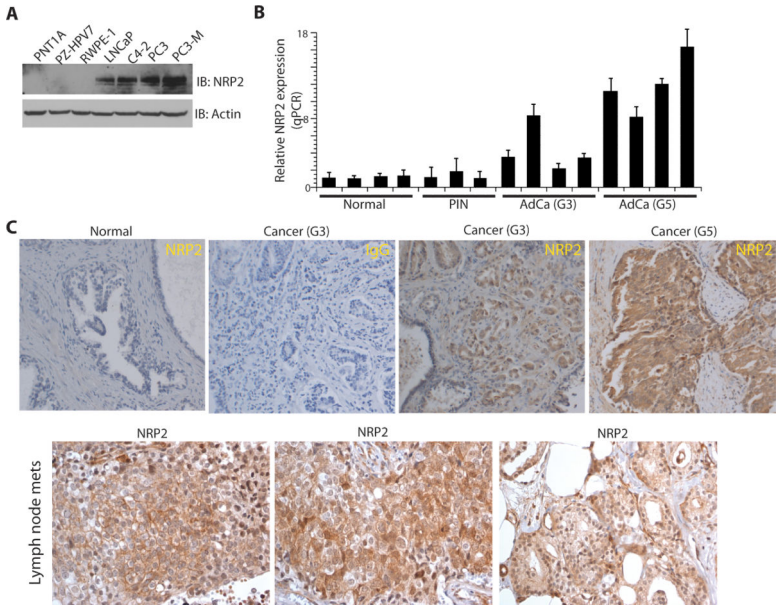

Figure 1. Neuropilin-2 expression is associated with prostate cancer progression

(A) Normal (PNT1A, PZ-HPV7 and RWPE-1) or prostate cancer (LNCaP, C4-2, PC3 and PC3M) cell lines were immunoblotted using Abs to NRP2 or actin. (B) Expression of NRP2 mRNA was quantified by qPCR in microdissected sections from normal glands, PIN, grade 3 and grade 5 prostate cancer specimens. (C) Specimens of normal prostate gland, Gleason grade 3 and grade 5 carcinoma and lymph node metastases were immunostained with a NRP2 Ab or a control IgG.

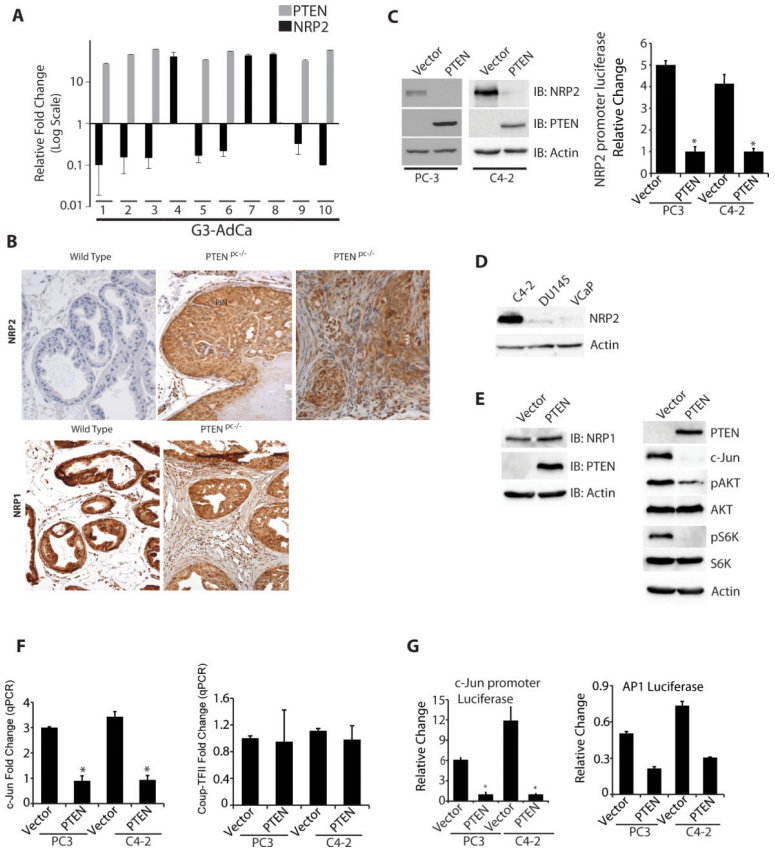

Figure 2. PTEN loss induces NRP2 and c-Jun

(A) Microdissected specimens of tumor cells from Gleason grade 3 prostate cancer specimens were analyzed for NRP2 and PTEN expression by qPCR. (B) Wild-type or PTEN$^{pc-/-}$ prostates [PIN (6 wks) and carcinoma (20 wks)] were stained with either a NRP2 or a NRP1 Ab. NRP2 expression was not detected in the wild-type prostate (n=4), but there is significant NRP2 expression in PIN lesions and carcinomas of PTEN$^{pc-/-}$ mice (n=4). In contrast, NRP1 is expressed in both normal prostate epithelium and carcinomas. (C) PC3 or C4-2 cells were transfected with either a PTEN-expressing vector or vector control, and extracts were immunoblotted for PTEN, NRP2 and actin (left blot). These cells were also transfected with a luciferase reporter construct containing the NRP2 promoter. Luciferase activity was measured and normalized to Renilla (right graph). (D) Extracts from C4-2, VCaP and DU145 cells were immunoblotted for NRP2 and actin. (E) PC3 cells were transfected with either a PTEN-expressing vector or vector control, and extracts were immunoblotted for PTEN, NRP1 and actin (left blot) or for key signaling molecules (right blot). (F) PC3 or C4-2 cells were transfected with either a PTEN-expressing vector or vector control, and the expression of c-Jun (left graph) and Coup-TFII mRNA (right graph) was quantified by qPCR. (G) PC3 or C4-2 cells expressing either PTEN or vector control were transfected with reporter constructs containing either the c-Jun promoter or AP1 reporter. Luciferase activity was measured and normalized to Renilla.

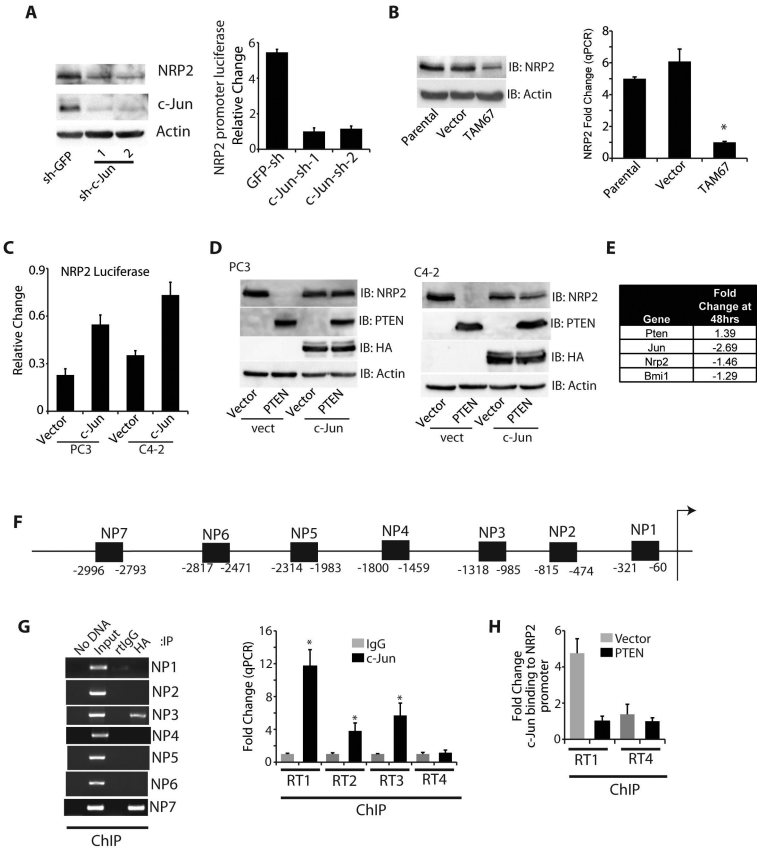

Figure 3. c-Jun regulates NRP2 expression

(A) PC3 cells were transfected with either a GFP-shRNA or two independent c-Jun shRNAs (1 and 2), and extracts were immunoblotted for NRP2, c-Jun and actin (left blot). A NRP2 promoter reporter construct was expressed in these cells and luciferase activity was normalized to Renilla (right graph). (B) PC3 cells were transfected with either TAM67 (a dominant negative c-Jun construct) or vector control. Extracts were immunoblotted for NRP2 and actin (left blot), and NRP2 mRNA expression was quantified by qPCR (right graph). (C) A c-Jun expression vector or control was expressed in either PC3 or C4-2 cells along with a NRP2 promoter reporter construct, and luciferase activity was normalized to Renilla. (D) PC3 or C4-2 cells expressing either PTEN or vector control were transfected with c-Jun (HA tagged) and protein extracts were immunoblotted for NRP2, PTEN, HA and actin. (E) Variation in the expression of PTEN, c-Jun, NRP2 and Bmi-1 upon PTEN induction (48 hours) in *Pten*$^{-/-}$ cells as described in Results. (F) Schematic representation of the NRP2 promoter. The arrow indicates the transcriptional start site. Highlighted boxes (NP1-7) represent the primers used to amplify the ChIP DNA using semi-quantitative PCR in G. (G) PC3 cells were transfected with an HA-c-Jun construct and ChIP was performed using an HA antibody or rat IgG to identify c-Jun binding sites on the *NRP2* promoter. The precipitated DNA was amplified by PCR using primers specific for NP regions 1 to 7 (left gel) and the results were quantified by qPCR (right graph). The RT1-4 primers used for qPCR described in Figure S8. (H) The effect of PTEN expression on c-Jun binding to the *NRP2* promoter was assessed by ChIP and quantified by qPCR.

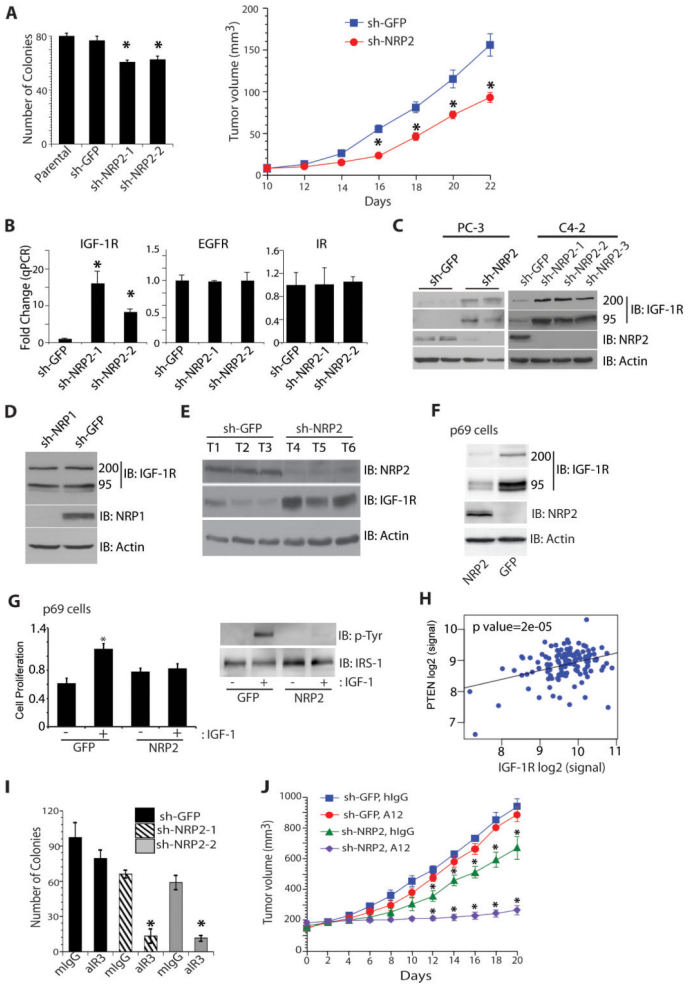

Figure 4. NRP2 represses IGF-IR expression and signaling

(A) PC3 cells were either not transfected (parental) or transfected with either a GFP-shRNA (sh-GFP) or two independent NRP2 shRNAs (sh-NRP2-1 and sh-NRP2-2) and analyzed for growth in soft agar (left graph). These transfectants (sh-GFP or sh-NRP2) were implanted in immunocompromised mice and xenograft growth was measured on alternate days (n=8) (right graph). (B) Expression of IGF-IR, EGFR and insulin receptor (IR) mRNA was quantified in PC3 transfectants (sh-GFP, sh-NRP2-1 and sh-NRP2-2) by qPCR. (C) Extracts from PC3 (sh-GFP or sh-NRP2) and C4-2 (sh-GFP or sh-NRP2) transfectants were immunoblotted for IGF-IR, NRP2 and actin. (D) Extracts from PC3 transfectants (GFP-sh or NRP1-sh) were immunoblotted for IGF-IR, NRP1 and actin. (E) Extracts from PC3 xenograft tumors (sh-GFP or sh-NRP2) were immunoblotted for NRP2, IGF-IR and actin. (F-G) Prostate epithelial cells (p69) were transfected with either NRP2 or GFP, and extracts were immunoblotted for IGF-1R, NRP2 and actin (F). These transfectants were also analyzed for cell proliferation in response to IGF-1 using the MTT assay (middle graph). They were also serum-deprived for 12 hours and stimulated with IGF-1 (50 ng/ml) for 10 minutes. Cell extracts were used to immunoprecipitate IRS-1 and immunoblotted for phospho-tyrosine (p-Tyr) or IRS-1 (right blot). (H) A significant correlation (p value is 2×10^{-5}) in expression of PTEN and IGF-1R was observed in human prostate specimens

(n=128) as described in results. (I) PC3 transfectants (sh-GFP, sh-NRP2-1 and sh-NRP2-2) were analyzed for anchorage-independent growth in the presence of either hIgG or an IGF-IR Ab (αIR3, 1 mg/ml). (J) PC3 transfectants (sh-GFP, or sh-NRP2) were implanted in immuno-compromised mice. Mice were injected i.p. with either A12 (IGF-1R Ab) or IgG (40 mg/kg, thrice a week), once the tumor volume reached ~150mm^3. Xenograft growth was measured on alternate days. Two groups of mice (sh-NRP2 + hIgG and NRP2sh + A12) exhibited significant inhibition of tumor growth compared to the remaining two groups (GFPsh, hIgG and GFP-sh, A12). *p-value is less than 0.05. Eight tumors were analyzed for each group.

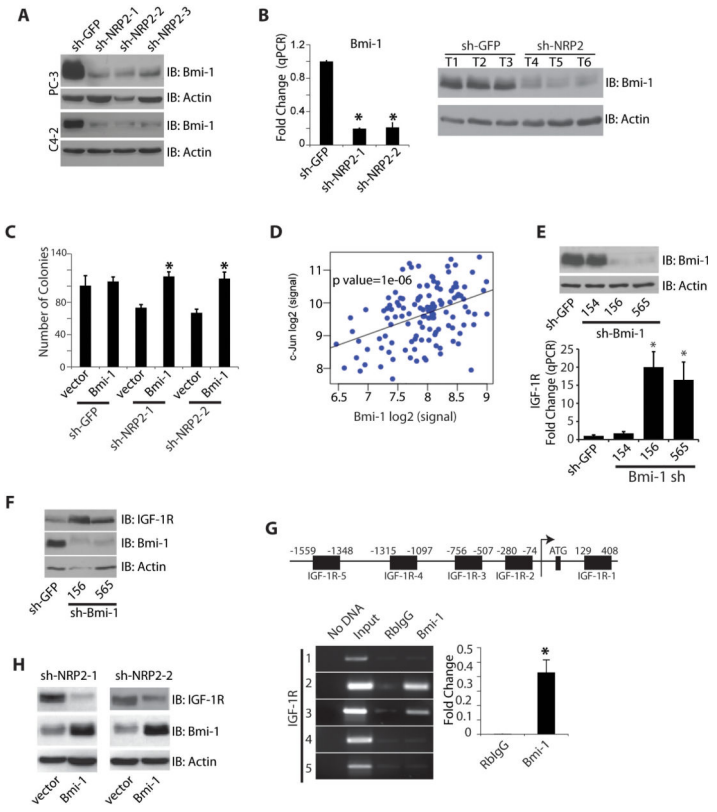

Figure 5. NRP2 sustains expression of Bmi-1, which represses IGF-1R transcription

(A-B) Bmi-1 expression was evaluated in PC3 and C4-2 transfectants (sh-GFP, sh-NRP2-1, sh-NRP2-2 and sh-NRP2-3) by immunoblotting (A) and qPCR (B, left graph). Extracts from PC3 xenograft tumors (sh-GFP or sh-NRP2) were immunoblotted for Bmi-1 and actin (B, right blot). (C) PC3 transfectants (sh-GFP, sh-NRP2-1 or sh-NRP2-2) were infected with lentivirus particles expressing either GFP or Bmi-1 and analyzed for growth in soft agar. Expression of Bmi-1 increases anchorage-independent growth. (D) A significant correlation (p value is 1×10^{-6}) in the expression of c-Jun and Bmi-1 was observed in human prostate specimens (n=128) as described in results. (E) PC3 transfectants (sh-GFP or sh-Bmi-1) cells were immunoblotted for Bmi-1 and actin (upper blot). PC3 transfectants (sh-GFP, sh-Bmi-154, sh-Bmi-156 and sh-Bmi-565) were analyzed for IGF-1R mRNA by qPCR. Note: sh-Bmi-1-154 did not decrease Bmi-1 expression and showed no effect on IGF-1R mRNA (lower graph). (F) PC3 transfectants (sh-GFP, sh-Bmi-156 and sh-Bmi-565) were immunoblotted for Bmi-1, IGF-1R and actin. (G) ChIP analysis of Bmi-1 binding to the IGF-1R promoter. A schematic of the IGF-1R promoter with highlighted boxes (IGF-1R-1-5) representing the primers used to amplify the ChIP DNA by semi-quantitative PCR. The arrow indicates the transcriptional start site and ATG indicates the translation start codon. ChIP was performed using a Bmi-1 antibody or rabbit IgG and precipitated DNA was amplified by PCR using primers specific for regions 1 to 5. Bmi-1 binding to the *IGF-1R* promoter was confirmed by qPCR. (H) PC3 transfectants (sh-NRP2-1 and sh-NRP2-2) were infected with lentivirus particles expressing either GFP or Bmi-1, and extracts were immunoblotted for IGF-1R, Bmi-1 and actin.

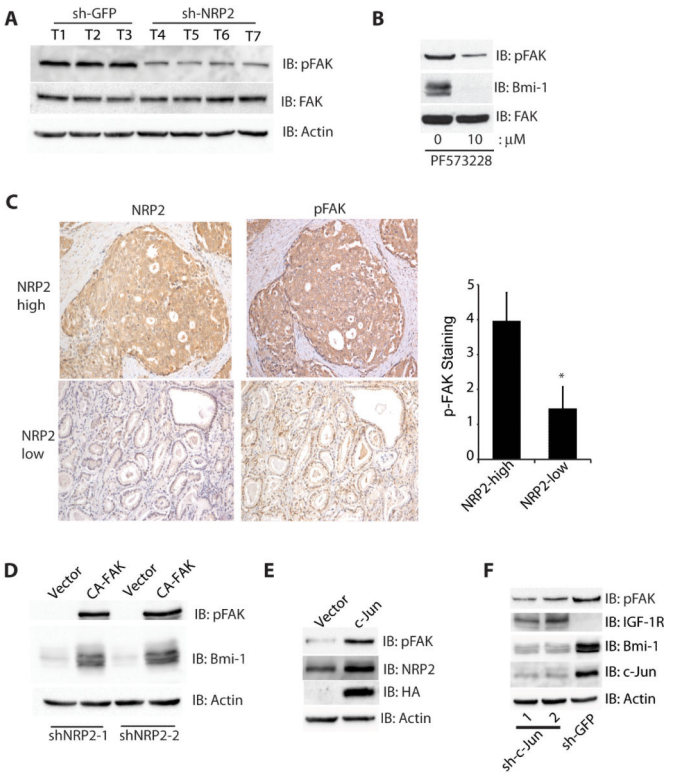

Figure 6. FAK mediates NRP2-stimulated Bmi-1 expression

(A) Extracts from PC3 xenograft tumors (sh-GFP or sh-NRP2) were immunoblotted for pFAK (pY397), total FAK and actin. (B) PC3 cells were incubated with a FAK inhibitor PF573228 (10 μM), and extracts were immunoblotted for pFAK, Bmi-1 and FAK. (C) Human prostate cancer specimens (n=24) were immunostained for NRP2 and pFAK (pY397). NRP2 staining was scored as either low (score 0 or 1) or high (score 2-5). pFAK staining was scored at a scale of 1 to 5. The graph summarizes the intensity of pFAK in NRP2-low and NRP2-high tumors. There is significantly higher pFAK in the NRP2-high tumors than in the NRP2-low tumors ($p= 0.00004$). (D) PC3 transfectants (sh-NRP2-1 and sh-NRP2-2) were transfected with either CA-FAK (K38A) or vector alone, and extracts were immunoblotted for pFAK (pY397), Bmi-1 and actin. (E) LNCaP cells were transfected with either c-Jun or vector, and immunoblotted for pFAK (pY397), NRP2, HA and actin. (F) PC3 cells were transfected with c-Jun shRNAs (1 and 2) or a GFP shRNA, and immunoblotted for pFAK (pY397), IGF-1R, c-Jun, Bmi-1 and actin.

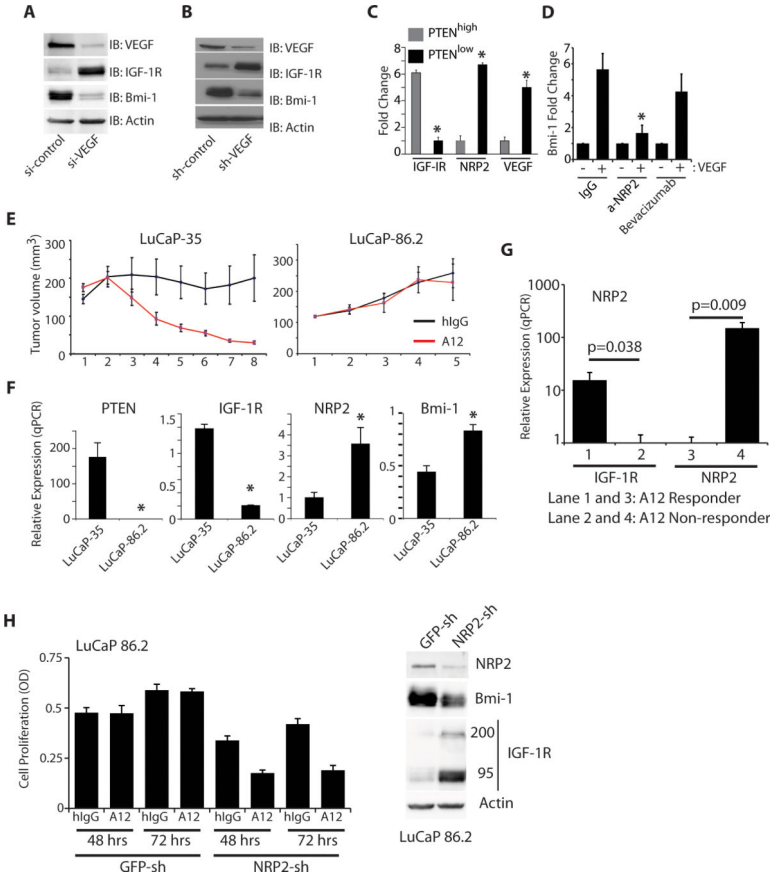

Figure 7. VEGF regulates Bmi-1 and IGF-1R expression

(A-B) PC3 cells were either transfected with VEGF siRNA Smartpool (A) or infected with a VEGF shRNA (B). Extracts were immunoblotted for VEGF, NRP2, Bmi-1 and actin. (C) Microdissected tumor cells from PTEN^{high} (n=6) or PTEN^{low} (n=6) prostate cancer specimens were analyzed for VEGF, NRP2 and IGF-1R mRNA expression by qPCR. PTEN expression correlates positively with IGF-1R, and negatively with NRP2 and VEGF expression. (D) PC3 cells expressing sh-VEGF were incubated with VEGF in the presence of control IgG, a NRP2 Ab or bevacizumab. Cells were analyzed for expression of Bmi-1 by qRT-PCR. NRP2 expression predicts response to IGF-1R therapy (E-H). (E) Graphs display the volume of LuCaP xenograft tumors (+/− SEM) of 10 castrated mice after A12 or human IgG treatment. (F) LuCaP xenografts (35 and 86.2) were analyzed for IGF-1R, NRP2, PTEN and Bmi-1 expression by qPCR. The A12 non-responder (86.2, PTEN-null) had significantly higher NRP2 and Bmi-1 expression than did the A12 responder. *p-value is less than 0.05. (G) IGF-1R and NRP2 expression was quantified by qPCR in 15 A-12 responder and 8 non-responder LuCaP xenografts. Data show 150-fold more NRP2 expression in the non-responders compared to responders and only a 10-fold increase in IGF-1R expression in the responders compared to the non-responders. (H) Freshly isolated cells from LuCaP 86.2 tumors were infected with lentivirus expressing either sh-GFP or sh-NRP2. Cell proliferation was measured in the presence of either hIgG or A12 up to 72 hours

using MTT assay (left graph) and the expression of NRP2, Bmi-1 and IGF-1R was assessed by immunoblotting (right blot).